Electronic Supplementary Information

Long-term effects of CeO_2 NPs on biological phosphorus removal mechanism of DPR-AGS in A/O/A SBRs

Xiaoying Zheng[1,2,*], Dan Lu[2], Yuan Zhang[2], Wei Chen[1,2], Mengqi Jin[2],

Xiaoyao Shao[2], Mengmeng Yang[2]

1. Ministry of Education Key Laboratory of Integrated Regulation and Resource Development on Shallow Lakes, Hohai University, Nanjing 210098, PR China

2. College of Environment, Hohai University, Nanjing 210098, PR China.

Corresponding author

Tel: 86-25-83786707

Fax: 86-25-83786707

E-mail: zhxyqq@hhu.edu.cn

The Number of Pages: 10

The Number of Tables: 6

The Number of Figures: 5

METHODS

Method 1. Determination of ROS Production and LDH

The intracellular ROS production was determined according to the literature (Wang et al., 2016). In short, AGS samples were first washed with phosphate buffer solution (PBS) three times; then the particles (wet weight 15 mg) were resuspended in 0.1 M phosphate buffer containing 20 M dichlorodihydrofluorescein acetate at 35±1 °C in the dark for 30 min; the particles were harvested by centrifugation and suspended in 0.1 M phosphate buffer and inoculated in a 96-hole plate. The fluorescein DCF generated was measured after 30 min using a microplate reader (Tecan InfiniteM200, Switzerland) with 485 nm excitation and 520 nm emission filters. LDH is used to characterize the integrity of the cell membrane, and the LDH level was determined according to previous research (Wang et al., 2016).

Method 2. Evaluation of the microbial community in the DPR-AGS

The extracted DNA samples were stored at -20 °C until use. Then, partial 16S rDNA based on high-throughput sequencing was used to determine the microbial diversity and composition of each AGS sample. PCR amplification was based on the primers 341F (CCTACGGGNGGCWGCAG) and 805R (GACTACHVGGGTATCTAATCC) in the V3-V4 region of 16S rDNA. Bacterial communities were measured by Illumina high-throughput sequencing technology, which was conducted by Sangon Biotech (Shanghai) Co., Ltd. The sequences were systematically classified using the RDP classifier and assigned to different levels. Besides, the phylogenetic relationships of each 16S rRNA gene sequence were analyzed by RDP classifier against the silva (SSU115) 16S rRNA database using a confidence threshold of 70%. Coverage, Shannon, Chao, ACE and Simpson indexes were generated in MOTHUR for each AGS sample. A Venn diagram with shared and unique OTUs was used to describe the similarities and differences between AGS samples at different CeO_2 NPs concentrations.

References:

Wang, S., Gao, M., Li, Z., She, Z., Wu, J., Dong, Z., Liang, G., Zhao, Y., Feng, G., Wang, X., 2016. Performance evaluation, microbial enzymatic activity and microbial community of a sequencing batch reactor under long-term exposure to cerium dioxide nanoparticles. *Bioresource Technology*, 220, 262.

TABLES

Table S1. Mass balance of CeO_2 NPs during wastewater treatment [a]

Influent (mg/L)	Effluent (mg/L)	Percentage in the reactor (%)
1	0.01 ± 0.003	99.0 ± 0.31
10	0.43 ± 0.005	95.7 ± 0.12

[a] Results are the averages and their standard deviations of triplicate tests.

Table S2. Effect of CeO_2 NPs concentration on the production of protein and polysaccharides contained in EPS[a].

CeO_2 NPs (mg/L)	PN	PS	EPS_{total}
0	90 ± 6.38	70 ± 4.86	160 ± 3.13
1	88 ± 4.12	75 ± 3.55	163 ± 3.55
10	108 ± 8.64	90 ± 6.74	198 ±5.98

[a] the data in the table gives the averages and their standard deviations, determined from triplicate measurements, in units of mg/g VSS.

Table S3. Chemical shifts and peak areas of the identified P species in ^{31}P NMR spectra of the PCA-NaOH and CER extracts of the DPR-AGS at the end of anaerobic stage (in 100 min).

		orthoP		Monoester-P		Diester-P		pyroP		End groups of polyP		Middle groups of polyP		Mean chain length of polyP
		Chemical shift (ppm)	Peak area (%)	Chemical shift (ppm)	Peak area (%)	Chemical shift (ppm)	Peak area (%)	Chemical shift (ppm)	Peak area (%)	Chemical shift (ppm)	Peak area (%)	Chemical shift (ppm)	Peak area (%)	
Cells	R0	5.31	7.12	2.57	13.64	0.36	15.15	-5.10	10.34	-4.51	20.43	-19.67 -20.33 -21.01	33.32	14.32
	R10	5.56	8.51	2.41	12.45	0.48	14.98	-5.45	10.12	-4.73	17.11	-19.52 -20.27 -21.38	36.83	17.16
EPS	R0	5.34	18.12					-5.01	10.45	-4.49	56.31	-20.34 -21.24	15.12	6.91
	R10	5.27	14.93					-4.96	10.64	-4.64	42.31	-20.42 -21.14	32.12	9.58

Table S4. Chemical shifts and peak areas of the identified P species in ^{31}P NMR spectra of the PCA-NaOH and CER extracts of the DPR-AGS at the end of aerobic stage (in 220 min).

		orthoP		Monoester-P		Diester-P		pyroP		End groups of polyP		Middle groups of polyP		Mean chain length of polyP
		Chemical shift (ppm)	Peak area (%)	Chemical shift (ppm)	Peak area (%)	Chemical shift (ppm)	Peak area (%)	Chemical shift (ppm)	Peak area (%)	Chemical shift (ppm)	Peak area (%)	Chemical shift (ppm)	Peak area (%)	
Cells	R0	5.83	9.85	2.31	8.53	0.34	10.73	-5.03	9.42	-4.41	14.42	-19.65 -20.65 -21.60	46.05	22.83
	R10	5.57	11.65	2.47	11.91	1.13	7.14	-5.01	10.56	-4.58	19.09	-19.52 -20.23 -21.38	39.65	16.75
EPS	R0	5.34	25.31					-5.05	6.52	-4.37	30.64	-20.26 -21.38	41.53	12.82
	R10	5.23	19.36					-4.90	7.41	-4.52	28.48	-20.13 -21.42	45.05	14.06

Table S5. Chemical shifts and peak areas of the identified P species in ^{31}P NMR spectra of the PCA-NaOH and CER extracts of the DPR-AGS at the end of anoxic stage (in 330 min).

		orthoP		Monoester-P		Diester-P		pyroP		End groups of polyP		Middle groups of polyP		Mean chain length of polyP
		Chemical shift (ppm)	Peak area (%)	Chemical shift (ppm)	Peak area (%)	Chemical shift (ppm)	Peak area (%)	Chemical shift (ppm)	Peak area (%)	Chemical shift (ppm)	Peak area (%)	Chemical shift (ppm)	Peak area (%)	
Cells	R0	5.69	6.95	2.59	8.65	0.42	9.18	-4.87	9.33	-4.53	11.58	-19.37 -20.41 -21.23	54.31	30.98
	R10	5.56	7.51	2.44	10.46	1.10	7.97	-4.93	10.12	-4.43	18.1	-19.62 -20.37 -20.88	42.84	18.33
EPS	R0	5.37	21.31					-5.05	8.42	-4.46	34.14	-20.64 -21.12	26.13	9.61
	R10	5.23	18.64	2.38	4.35	0.41	7.23	-4.90	9.61	-4.64	25.32	-20.14 -21.05	35.43	13.06

Table S6. Percentage of representative abundance of genera (phosphorus removal bacteria) in R0 (0 mg/L), R1 (1 mg/L) and R10 (10 mg/L).

Genus	R0 (%)	R1 (%)	R10 (%)
Comamonadaceae	7.12	6.89	6.23
Rhodocyclaceae	4.98	4.71	4.06
Pseudomonas	5.02	6.15	2.05
Acinetobacter	8.19	7.45	3.42
Azoarcus	6.36	5.56	1.31
Candidatus Hydrogenedens	2.12	2.32	2.17
Comamonas	3.46	3.12	3.25
Thauera	2.68	2.08	0.38
Dechloromonas	4.68	7.65	9.95
Defluviicoccus	3.08	3.05	7.06

FIGURES

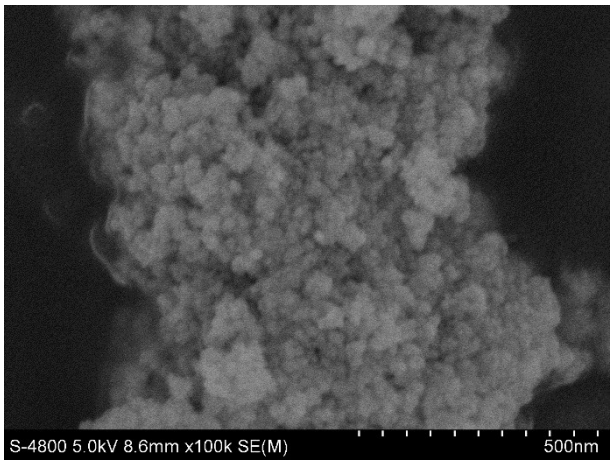

Figure S1. Scanning electron micrograph (SEM) image of CeO_2 NPs used in this study

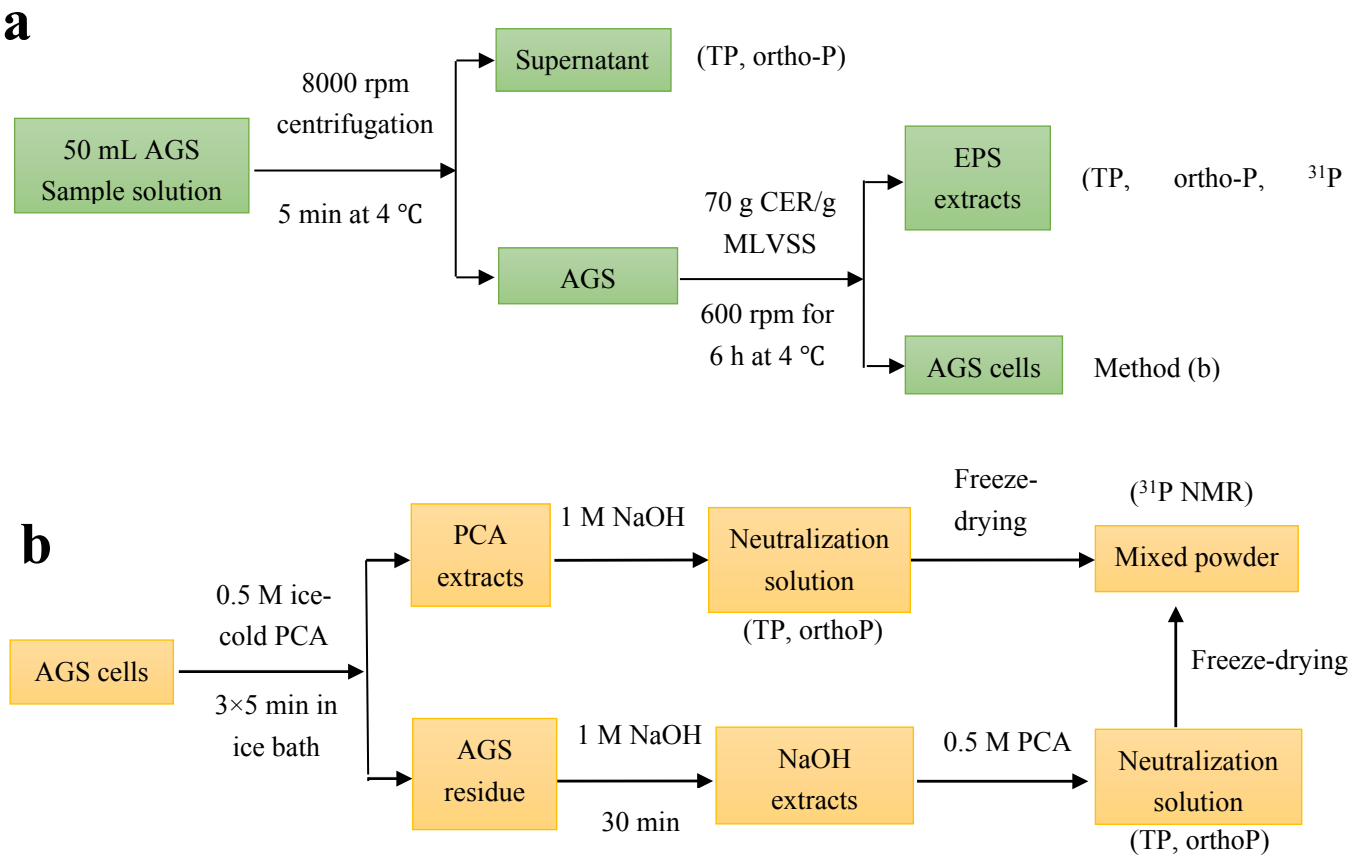

Figure S2 Schematic diagrams for the fractionation and characterization of various forms of P in EPS (a) and AGS residue (b).

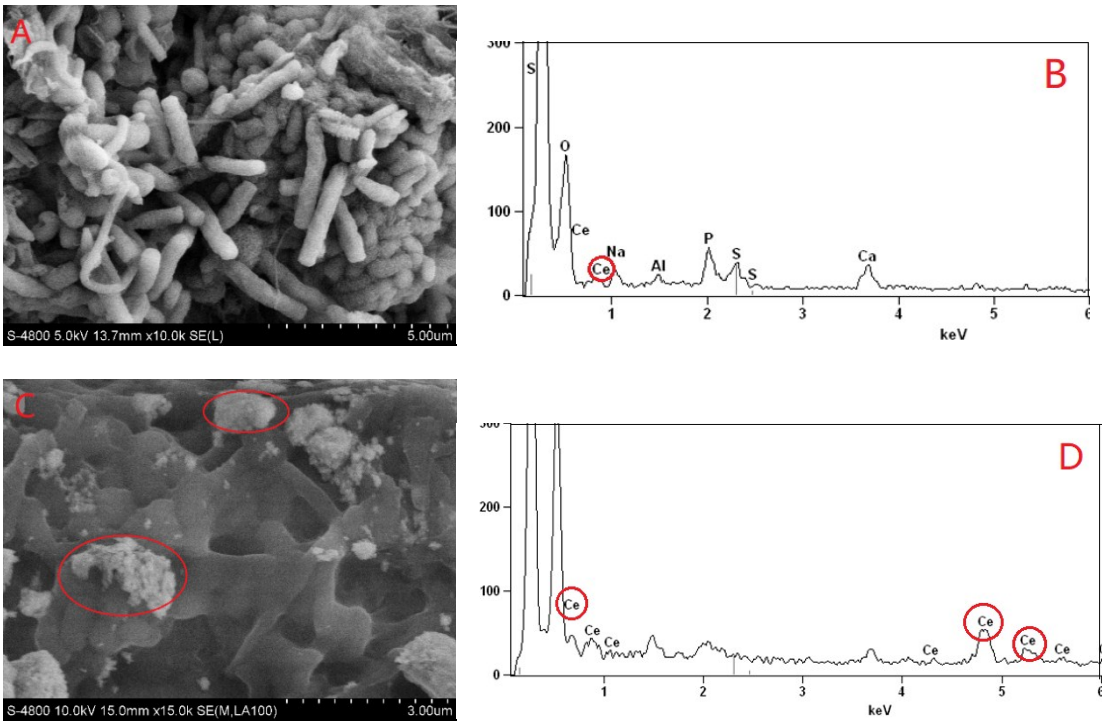

Figure S3. SEM images and EDX analysis of DPR-AGS exposed to different concentrations of CeO_2 NPs. The CeO_2 NPs concentrations of R0 (A, B) and R10 (C, D) were 0 and 10 mg/L respectively.

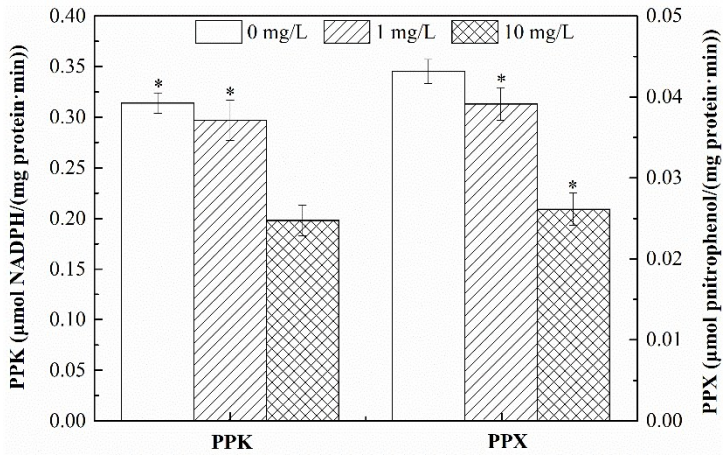

Figure S4. Microbial enzymatic activities of DPR-AGS at different CeO_2 NPs concentrations: PPK and PPX. Asterisks indicate statistical differences ($p < 0.05$) from the controls. Error bars represent standard deviations of triplicate measurements.

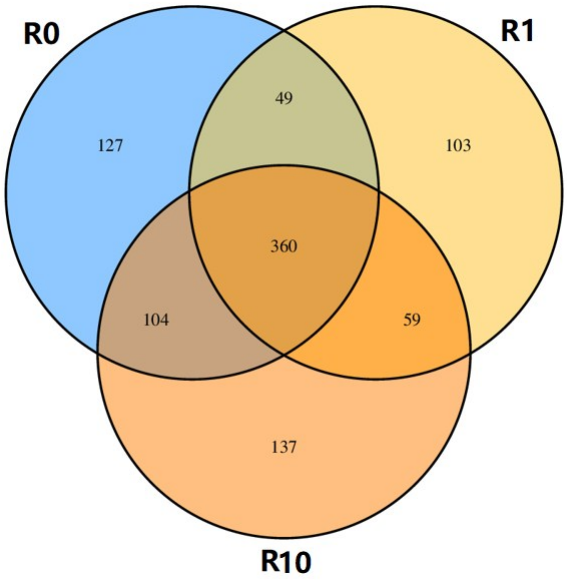

(a) Venn diagram of OTUs in R0, R1 and R10 samples.

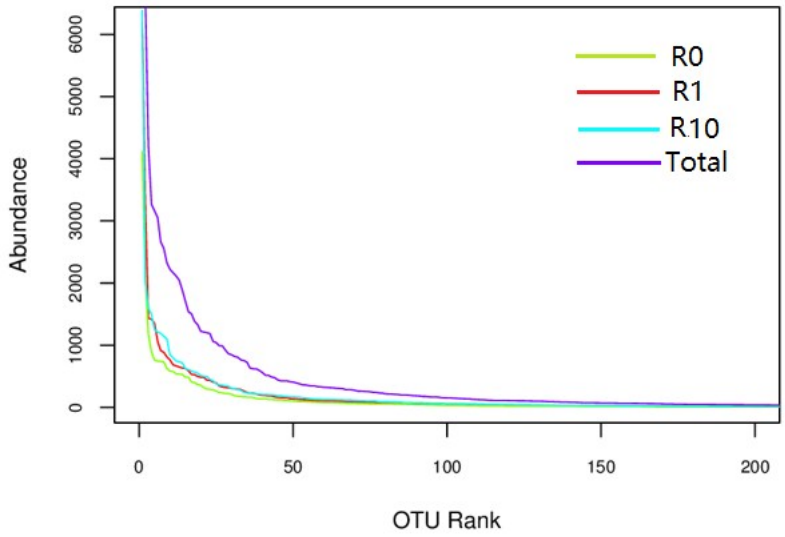

(b) Rank abundance curve

Figure S5. Venn diagram of OTUs **(a)** and rank abundance curve **(b)** of R0 (0 mg/L), R1 (1 mg/L) and R10 (10 mg/L) samples.